This is a preprint, the final version is subject to change, of the American Mineralogist (MSA)
Cite as Authors (Year) Title. American Mineralogist, in press.
(DOI will not work until issue is live.) DOI: http://dx.doi.org/10.2138/am-2015-5285

Revision 1

Experimental confirmation of high temperature silicate liquid immiscibility in multicomponent ferrobasaltic systems

Tong Hou[1,2*], Ilya V. Veksler[2,3,4]

1. State Key Laboratory of Geological Process and Mineral Resourses, China University of Geosciences, Beijing, 100083, China
2. GFZ German Research Center for Geosciences, Telegrafenberg, D-14473 Potsdam, Germany
3. Department of Mineralogy, Technical University Berlin, Ackerstrasse 71–76, Berlin 13555, Germany
4. Perm State University, Geological Department, Bukireva 15, 614990 Perm, Russia

Corresponding author: Dr. Tong Hou

E-mail address: thou@cugb.edu.cn

Address: Room 818, Run Run Shaw Building

29 Xueyuan Road, Haidian District, Beijing, 100083, China

* Corresponding author. E-mail: thou@cugb.edu.cn

Abstract

Here we report the results of an experimental study aimed at testing the existence of stable, super-liquidus immiscibility between silica-rich and Fe-rich multicomponent melts at temperatures above 1100 °C. Four pairs of the potentially immiscible compositions were tested in a one-atmosphere gas-mixing furnace (Ar/H_2-CO_2 gas mixture) at 1150 and 1200 °C and at the oxygen fugacity corresponding to that of the QFM buffer. Pre-synthesized pairs of the silica-rich and Fe-rich starting compositions were loaded in Pt wire loops, fused separately at 1300 °C, then brought in contact and kept at constant experimental temperature for more than 24 hours. Three pairs of compositions out of four used in this study did not mix. Some temperature-dependent chemical re-equilibration was observed in the Fe-rich liquid phase but, in the cases of immiscibility, the two liquids remained compositionally distinct and showed sharp compositional gradients at contacts. One pair of liquids crystallized some tridymite, whereas the other compositions were clearly above the liquidus. Overall, the results of the experiments are in good agreement with the earlier centrifuge study and confirm the existence of stable, super-liquidus immiscibility in some Fe-rich basaltic-andesitic compositions at temperatures up to 1200 °C.

Keywords: experimental petrology; silicate liquid immiscibility; ferrobasaltic; multicomponent silicate melts

Introduction

Liquid immiscibility between ferrobasaltic and rhyolitic melts in a broad compositional range of natural magmas has been considered as a potentially important mechanism of magma differentiation (Charlier et al. 2013; Kamenetsky et al. 2013; Namur et al. 2012; Thompson et al. 2007; Veksler et al. 2007; Veksler and Charlier 2015). The existence of silicate liquid immiscibility in natural lavas of ferrobasaltic-ferrodacitic composition has long been recognized (e.g., Roedder 1992 and Philpotts 1982), and in recent years traces of immiscibility and liquid-liquid fractionation have been found in plutonic rocks in a number of mafic layered intrusions worldwide, such as immiscible silica- and Fe-rich melt inclusions in apatite and late-stage reactive microstructures (Jakobsen et al. 2005, 2011; Holness et al. 2011; Namur et al. 2012; Veksler and Charlier 2015). Stable coexistence of Fe-rich and silica-rich immiscible liquids in equilibrium with typical gabbroic mineral assemblages has been reproduced in numerous experiments (Charlier and Grove 2012; Dixon and Rutherford 1979; Longhi 1990; Philpotts and Doyle 1983) but, with only few exceptions (e.g., Roedder and Weiblen 1970; Krasov and Clocciatti 1979), unmixing of ferrobasaltic melts has been documented only at temperatures close to the liquidus of melts that have low liquidus temperatures, usually below 1020-1040 °C. The existence of high-temperature, super-liquidus silicate liquid immiscibility at temperatures up to 1200 °C has been proposed for some multicomponent ferrobasaltic-ferroandesitic compositions on the basis of centrifuge experiments (Veksler et al. 2006, 2007), but the evidence and interpretation of experimental results were challenged by Philpotts (2008) who argued that the

products of centrifuge experiments were metastable phases formed during quenching. The results of centrifuge experiments were indeed questionable because phase separation in many runs did not develop beyond the formation of sub-micron emulsions, and interpretation of such emulsions and opalescent glasses has been contentious (e.g., Visser and Koster van Groos 1976, 1977; Roedder 1977; Freestone and Hamilton 1977). It has been pointed out (Veksler et al. 2008a,b, 2010) that the protracted stability of the emulsions in the case of stable immiscibility may be due to low interfacial tension between the immiscible liquids, but researchers who have doubted the existence of stable immiscibility in natural ferrobasaltic compositions above 1040 °C seem to remain unconvinced (Kamenetsky et al. 2013)

The debate about the extent of silicate liquid immiscibility to higher temperatures in multicomponent compositions has important implications for natural magmatic systems, and it would be good to resolve it by experimental means despite the kinetic obstacles encountered in previous studies (Veksler et al. 2006, 2007, 2008a,b). It is a common practice in experimental petrology to test thermodynamic equilibrium by conducting direct and reverse experiments. A reverse approach to equilibrium, as opposed to the centrifuge experiments, would be to see whether two pre-synthesized immiscible liquid compositions do or do not mix at long exposure times in a conventional static setup. In the original centrifuge study, Veksler et al. (2007) tried the reverse approach but the results were poorly reproducible and inconclusive. To avoid metastable immiscibility, here we report the results of a new study, in which we used two beads of glass (Fe-rich and silica-rich) touching each other in the experiment and achieved good reproducibility of high-temperature immiscibility at exposure times of 24 h or longer. After making minor modifications to the reverse static setup used by Veksler et al. (2007) we have tested immiscibility for a few compositions

used in the original centrifuge study and two new ones, and confirmed the existence of stable immiscibility at temperatures up to 1200 °C in three cases out of four.

Experimental and analytical methods

Preparation of starting mixtures

Compositions and sources for the four pairs of the potentially immiscible compositions (MZ, RY, KC and PZH) are listed in Table 1. All the starting materials were synthesized by fusion in platinum crucibles of carefully weighed and mixed reagent-grade chemicals [SiO_2, Al_2O_3, MgO, TiO_2, $CaCO_3$, Na_2CO_3, K_2CO_3 and $Ca_3(PO_4)_2$]. To avoid strong oxidation and Fe losses to the crucibles, Fe-free glasses were first prepared by repeated fusions in an electric furnace once at 900 °C, and then twice at 1400 °C. The Fe-free glasses were then crushed to fine powders (grain size less than 3 μm), and mixed and ground with reagent-grade FeO in an agate mortar under acetone. The resulting powders of the glass-FeO mixtures were used as starting materials for the experimental charges

Experimental technique

The experiments were conducted at GeoForschungsZentrum (GFZ) Potsdam, Germany in a 1-atm vertical tube furnace (Vertical Gero Furnace Alsint tube type) in which oxygen fugacity (f_{O2}) was controlled by H_2/Ar-CO_2 gas mixtures. Gas flow was regulated by digital Brooks mass flow controllers and a $PtRh_6$-$PtRh_{30}$ (type B) thermocouple was used for temperature measurements. The thermocouple had

115 previously been calibrated against the melting point of gold (1064 °C).
116 Yttrium-stabilized zirconia electrolyte ($SIRO_2$) manufactured by Ceramic Oxide
117 Fabricators Pty. Ltd (Victoria, Australia) was used for the f_{O2} measurements inside the
118 furnace. Uncertainties of the cited log f_{O_2} values and the temperature do not exceed
119 ±0.2 and ±2 °C, respectively.

120 Fine powders of the Fe-rich and silica-rich reactant mixtures moistened with a
121 drop of water and some water-soluble organic binder were loaded in separate Pt wire
122 loops about 3 mm in diameter, fused at 1300 °C and f_{O_2} corresponding to that of the
123 QFM buffer, and subsequently quenched in air. Preheating and fusion of the
124 potentially immiscible liquid pairs in the separate wire loops was the key modification
125 which we made to the experimental procedure used by Veksler et al. (2007), who had
126 loaded both starting compositions into the same loop. Pre-fused pairs of the Fe-rich
127 and silica-rich glass beads were then suspended in a new position, in contact with
128 each other and kept at constant experimental temperature (1150 °C or 1200 °C) for at
129 least 24 hours. At the end of the run, samples were quenched in air in a few seconds.

130 *Electron microprobe analyses*

131 Run products were mounted in epoxy, ground and polished, and studied by
132 electron microprobe at the GeoForschungsZentrum Potsdam using a JEOL
133 Hyperprobe JXA-8500F in wavelength-dispersive spectrometry (WDS) mode at 15
134 kV accelerating voltage and 15 nA beam current with spot sizes ranging from 10 to 15

μm depending on the properties and compositions of the analyzed materials. Counting time for all the elements was set to 20 s on peak and 10 s on background. The following synthetic and natural standards were used for the calibration: orthoclase (Al and K), rutile (Ti), wollastonite (Si and Ca), albite and jadeite (Na), apatite (P), hematite (Fe), diopside and periclase (Mg). The precision for oxide concentrations is better than 1%.

Compositional mapping of a sample (PZH1200) for calcium was conducted using a highly sensitive four-segment backscattered electron (BSE) detector. We used the electron microprobe combined with X-ray, backscattered electron and cathodoluminescence (CL) maps. By scanning over a specified target area, CL wavelength and X-ray element distribution maps are acquired in parallel, enabling direct comparison between elemental concentrations and textural features.

Results

As explained in the introduction, the idea of the reverse experiments was to see if the pre-synthesized pairs of the Fe-rich and silica-rich liquid droplets would mix when held for more than 24 hours in contact with each other at constant temperature and fO_2 close to the QFM buffer. Mixing was supposed to be by chemical diffusion. However, some minor mechanical stirring of the liquids due to wetting and gravity forces was unavoidable, especially at the very beginning of the run. Surface tension merged two droplets into one and the buoyant silica-rich liquid usually floated up and

positioned itself on top of the denser and less viscous Fe-rich liquid.

In summary, one pair of compositions (labeled MZ in Table 1) completely mixed in both runs at 1150 °C and 1200 °C, which we take to indicate that the run durations were long enough to expect complete mixing by diffusion for all compositions if the two liquids were actually miscible. The other three pairs of the starting compositions did not. In these latter cases, the two liquids remained compositionally distinct and showed sharp chemical gradients at the contacts (Fig. 1). One pair of liquids (KC) crystallized some tridymite (Fig. 1b), whereas the other compositions were clearly above the liquidus. Tridymite crystallization in the RY compositions was also observed in the centrifuge experiments by Veksler et al. (2007) and the results of the direct and reverse experiments appear to be in a good agreement in this respect.

Electron microprobe analyses of all the run products are presented in the supplementary data set. The analyses of those samples that did not mix completely showed that liquid compositions, and especially the compositions of the Fe-rich phases, significantly changed in comparison with the starting compositions. Partial dissolution of the silica-rich liquid *Lsi* in the Fe-rich liquid *Lfe* was observed in all the runs in which the liquids did not mix completely. After the runs, unmixed *Lfe* compositions contained 53-56 wt. % SiO_2 (Table 2) instead of 38-50 wt. % SiO_2 in the starting *Lfe* mixtures (Table 1) and compositional contrast decreased for all the other major components. Mutual solubility of the melts with starting compositions RY and KC appears to increase with temperature, whereas the conjugate *Lfe* and *Lsi* melts with the starting mixture PZH were practically unchanged at 1150 °C and 1200 °C (Table 2). Losses of Fe into the Pt wire loops and losses of more volatile components by evaporation appear to be insignificant, except for phosphorus in the P_2O_5-rich mixtures RY, where P_2O_5 contents decreased by more than 50 % relative to the

concentrations in the starting reactant mixtures.

Discussion

In our view, the results of this study strongly support the existence of stable liquid immiscibility in some multicomponent, geologically relevant aluminosilicate compositions at temperatures up to 1200 °C. Except the complete mixing between the starting compositions MZ, the results are generally in good agreement with the earlier centrifugation study by Veksler et al. (2007). The coexisting immiscible liquid compositions in this study and in the centrifuge experiments are not exactly the same, but some compositional differences should be expected in view of the very different redox conditions in the direct centrifuge and the reverse static experiments (below the IW and at the FMQ buffers, respectively). Contacts between the immiscible liquids are not razor-sharp menisci but they are somewhat blurred. Diffuse contacts between the immiscible liquids have been also observed in some direct static experiments (e.g., Longhi 1990; Charlier and Grove 2012) and such textures have been interpreted as a result of ineffective phase separation and sluggish chemical diffusion. In the case of reverse "mixing" experiments, which is discussed here, diffuse contacts probably formed at the start of the static runs when the liquid droplets were moved and deformed by the forces of surface tension and gravity. Stirring by convection in the low-viscosity Fe-rich liquid may be another reason for the formation of diffuse contacts. If the liquids were close to chemical equilibrium, gradients of chemical potentials of major components were probably very low across the diffuse contacts. Therefore, sharpening by chemical diffusion of the contacts initially blurred by mechanical stirring may require much a longer time than the exposure times of our experiments. Nevertheless, the same result for the MZ sample, i.e. mixing, at two

different temperatures was observed, whereas all the other samples remained unmixed for two temperatures. Therefore, we believe that MZ was not just more thoroughly mechanically mixed (by chance) than the other three samples, but that the observations indicate differences in miscibility for these different compositions.

Implications

Overall, the results of the experiments are in good agreement with the earlier centrifuge study (Veksler et al. 2007) and strongly support the existence of stable liquid immiscibility in some multicomponent, geologically relevant aluminosilicate, i.e. Fe-rich basaltic-andesitic compositions at temperatures up to 1200 °C. Take the example of the Panzhihua layered gabbros (Wang et al. 2013): based on the chemical composition of the daughter minerals, including plagioclase and clinopyroxene and the melt inclusion, we calculated the liquidus temperature of the immiscible melts in this system. Our results showed that the liquidus temperature is about 1000 °C. Thus, with temperature decreases, the compositions of the conjugate silicate liquids moved further apart along the solvus, consistent with the previous studies (Charlier and Grove 2012; Kamanetsky et al. 2013), but the upper limit (critical point) of the solvus of the tholeiitic system is moderately higher than previously thought. Thus, silicate liquid immiscibility in a broad compositional range of natural magmas could be considered as a potentially important mechanism of magma differentiation.

Acknowledgements

We are grateful to Olivier Namur and an anonymous reviewer, and the editor Ian Swainson for their thoughtful and constructive comments. Oona Appelt in Helmholtz Centre Potsdam GFZ German Research Centre for Geosciences is thanked for assistance with electron microprobe analysis. Parts of this work were supported by Chinese 973 program (2012CB416806), the "Fundamental Research Funds for the Central Universities," the 111 Project (B07011) and DFG grant VE 619/2-1. IVV also acknowledges support by Russian Science Foundation, grant No. 14-17-00200.

SIGNATURES

Tong Hou

Ilya Veksler

References

Charlier, B., and Grove, T.L. (2012) Experiments on liquid immiscibility along tholeiitic liquid lines of descent. Contributions to Mineralogy and Petrology, 164, 27–44.

Dixon, S., and Rutherford, M.J. (1979) Plagiogranites as late-stage immiscible liquids in ophiolite and mid-ocean ridge suites: an experimental study. Earth and Planetary Science Letters, 45, 45-60.

Freestone, I.C., and Hamilton, D.L. (1977) Liquid immiscibility in K_2O-FeO-Al_2O_3-SiO_2: Discussion. Nature, 267, 559.

Holness, M.B., Stripp, G., Humphreys, M.C.S., Veksler, I.V., and Nielsen, T.F.D. (2011) Silicate liquid immiscibility within the crystal mush: Late-stage magmatic microstructures in the Skaergaard Intrusion, East Greenland. Journal of Petrology, 52, 175-222.

Jakobsen, J.K., Veksler, I.V., Tegner, C., and Brooks, C.K. (2005) Immiscible iron- and silica-rich melts in basalt petrogenesis documented in the Skaergaard intrusion. Geology, 33, 885-888.

Jakobsen, J.K., Veksler, I.V., Tegner, C., and Brooks, C.K. (2011) Crystallization of the Skaergaard intrusion from an emulsion of immiscible iron- and silica-rich liquids: Evidence from melt inclusions in plagioclase. Journal of Petrology, 52, 345-373.

Kamenetsky, V.S., Charlier, B., Zhitova, L., Sharygin, V., Davidson, P., and Feig, S.

(2013). Magma chamber–scale liquid immiscibility in the Siberian Traps represented by melt pools in native iron. Geology, 41, 1091-1094.

Krasov, N.F., and Clocchiatti, R. (1979) Immiscibility in silicate melts and its possible petrogenetic importance, as shown by study of melt inclusions. Transactions (Doklady) of the USSR Academy of Science 248, 92-95.

Longhi, J. (1990) Silicate liquid immiscibility in isothermal crystallization experiments. Proceedings of the 20th Lunar and Planetary Science Conference, 13-24.

Namur O., Charlier B., and Holness M. (2012) Dual origin of Fe–Ti–P gabbros by immiscibility and fractional crystallization of evolved tholeiitic basalts in the Sept Iles layered intrusion. Lithos, 154, 100–114.

Philpotts, A.R. (1982) Compositions of immiscible liquids in volcanic rocks. Contributions to Mineralogy and Petrology, 80, 201–218.

Philpotts, A.R. (2008) Comments on: Liquid immiscibility and the evolution of basaltic magma. Journal of Petrology, 49, 2171–2175.

Philpotts, A.R., and Doyle, C.D. (1983) Effects of magma oxidation state on the extent of silicate liquid immiscibility in a tholeiitic basalt. American Journal of Science, 283, 967-985.

Roedder, E. (1977) Liquid immiscibility in K_2O-FeO-Al_2O_3-SiO_2: Discussion. Nature, 267, 558-559.

Roedder, E. (1992) Fluid inclusion evidence for immiscibility in magmatic

differentiation. Geochimica et Cosmochimica Acta, 56, 5-20.

Roedder, E., and Weiblen, P.W. (1970) Silicate liquid immiscibility in lunar magmas, evidenced by melt inclusions in lunar rocks. Science, 167, 641–644.

Thompson, A.B., Aerts, M., and Hack, A.C. (2007) Liquid immiscibility in silicate melts and related systems. Reviews in Mineralogy and Geochemistry, 65, 99-127.

Veksler, I.V., and Chariler, B. (2015) Silicate liquid immiscibility in layered intrusions. In: Charlier, B., Namur, O., Latypov, R., Tegner, C. (Eds.) Layered Intrusions. Springer, in press.

Veksler, I.V., Dorfman, A.M., Danyushevsky, l.M., Jakobsen, J.K., and Dingwell, D.B. (2006) Immiscible silicate liquid partition coefficients: Implications for crystal-melt element partitioning and basalt petrogenesis. Contributions to Mineralogy and Petrology, 152, 685–702.

Veksler, I.V., Dorfman, A.M., Borisov, A.A., Wirth, R., and Dingwell, D.B. (2007) Liquid immiscibility and evolution of basaltic magma. Journal of Petrology, 48, 2187-2210.

Veksler, I.V., Dorfman, A.M., Borisov, A.A., Wirth, R., and Dingwell, D.B. (2008a) Liquid immiscibility and evolution of basaltic magma. Reply to SA Morse, AR McBirney and AR Philpotts. Journal of Petrology, 49, 2177-2186.

Veksler, I.V., Dorfman, A.M., Rhede, D., Wirth, R., Borisov, A.A., and Dingwell, D.B. (2008b) Kinetics and the extent of liquid immiscibility in the system

K_2O-CaO-FeO-Al_2O_3-SiO_2. Chemical Geology, 256, 119–130.

Veksler, I.V., Kähn, J., Franz, G., and Dingwell, D.B. (2010) Interfacial tension between immiscible liquids in the system K_2O-FeO-Fe_2O_3-Al_2O_3-SiO_2 and implications for the kinetics of silicate melt unmixing. American Mineralogist, 95, 1679-1685.

Visser, W., and Koster van Groos, A.F. (1976) Liquid immiscibility in K_2O-FeO-Al_2O_3 -SiO_2. Nature, 264, 426-427.

Visser, W., and Koster van Groos, A.F. (1977). Liquid immiscibility in K_2O-FeO-Al_2O_3 -SiO_2: Reply to Roedder, Freestone and Hamilton. Nature, 267, 560.

Wang, K., Xing C., Ren, Z., and Wang, Y. (2013) Liquid immiscibility in the Panzhihua mafic layered intrusion: Evidence from melt inclusions in apatite. Acta Petrologica Sinica, 29, 3503-3518 (in Chinese with English abstract).

Figure caption

Figure 1. A series of back-scattered electron images of run products and electron microprobe compositional profiles across the contacts between silica-rich (*Lsi*) and Fe-rich (*Lfe*) glasses (a, RY1150; b, KC1150; c, PZH1200).

Figure 2. Ca distribution map in the sample PZH1200 showing a steep compositional gradient at the contact between two immiscible liquids (*Lfe* and *Lsi*).

330

331 **Table captions**

332 **Table 1.** Compositions of synthetic starting mixtures normalized to 100 wt.%.

333

334 **Table 2.** Representative compositions of experimental products based on electron

335 microprobe analyses of quenched glasses.

336

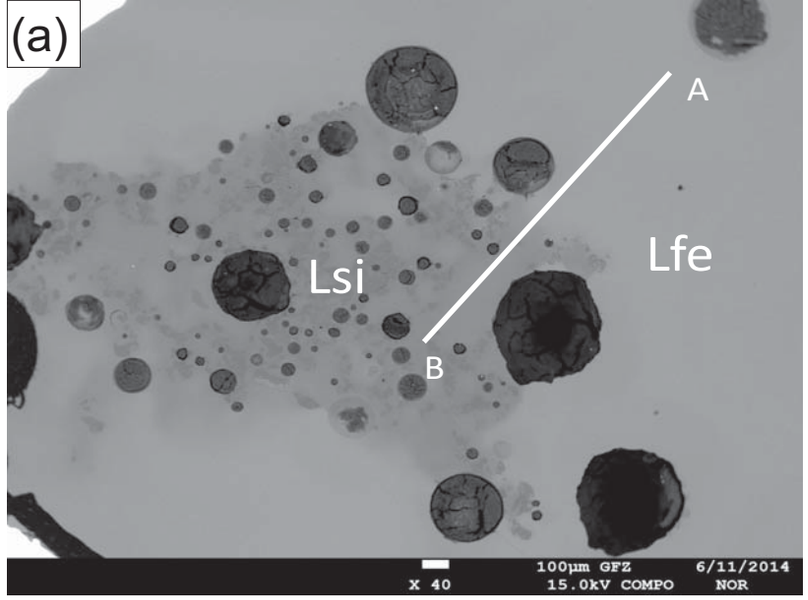
(a)
A
B
Lsi
Lfe
100µm GFZ
X 40
15.0kV COMPO
6/11/2014
NOR

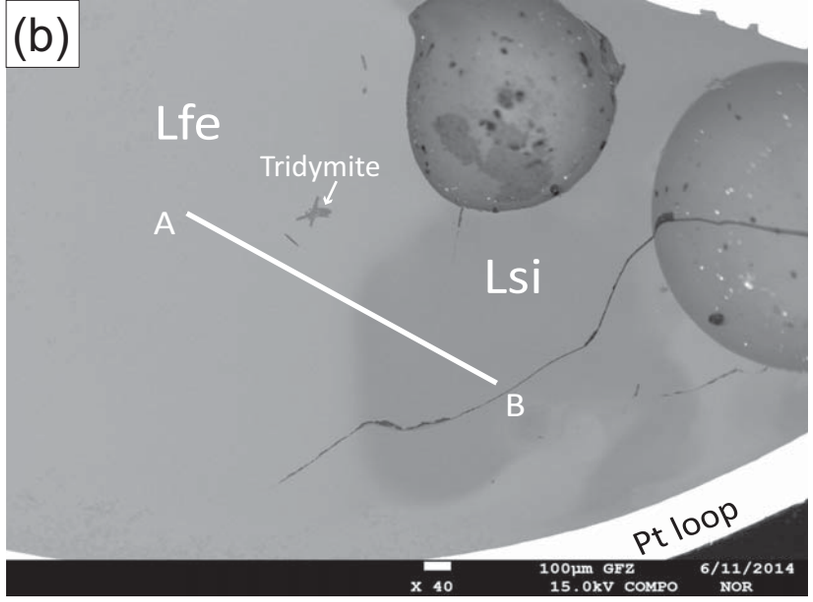
(b)
Lfe
Tridymite
A
Lsi
B
Pt loop
100µm GFZ
X 40
15.0kV COMPO
6/11/2014
NOR

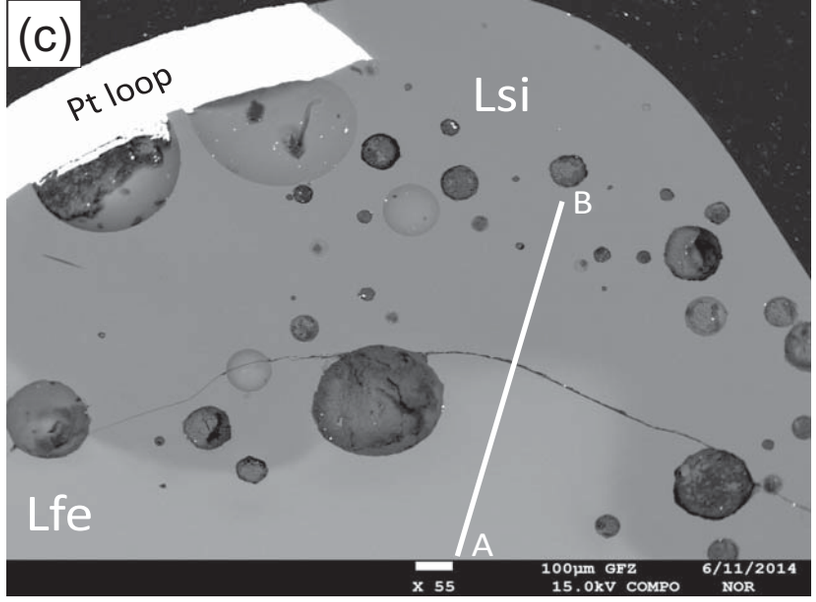
(c)
Pt loop
Lsi
B
Lfe
A
100µm GFZ
X 55
15.0kV COMPO
6/11/2014
NOR

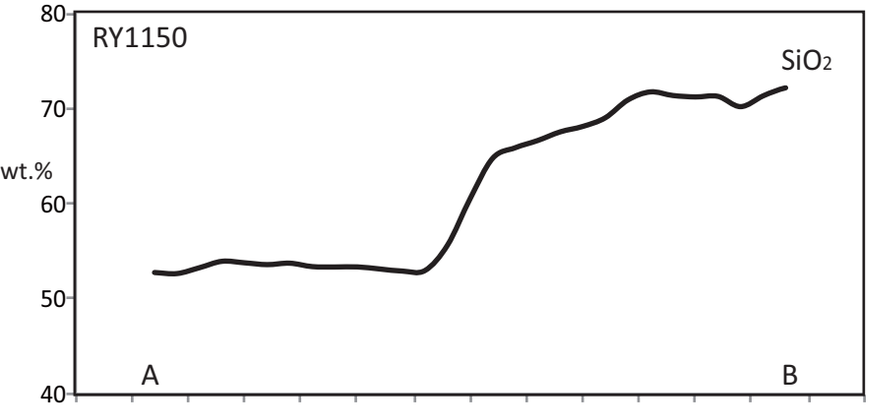
RY1150
SiO2
wt.%
80
70
60
50
40
A
B

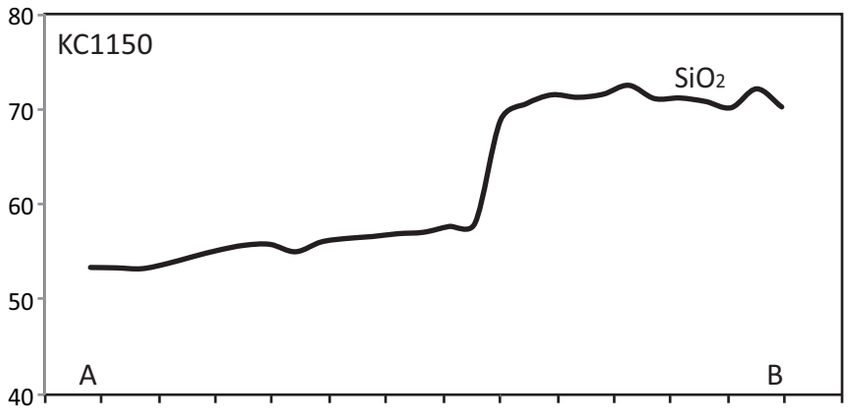
KC1150
SiO2
80
70
60
50
40
A
B

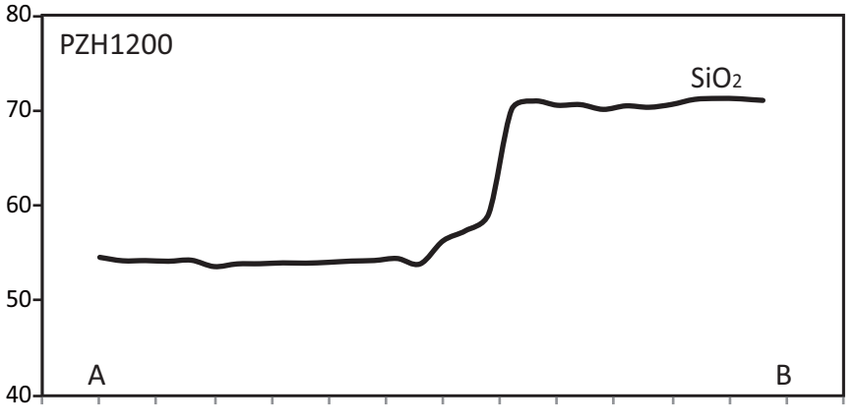
PZH1200
SiO2
80
70
60
50
40
A
B

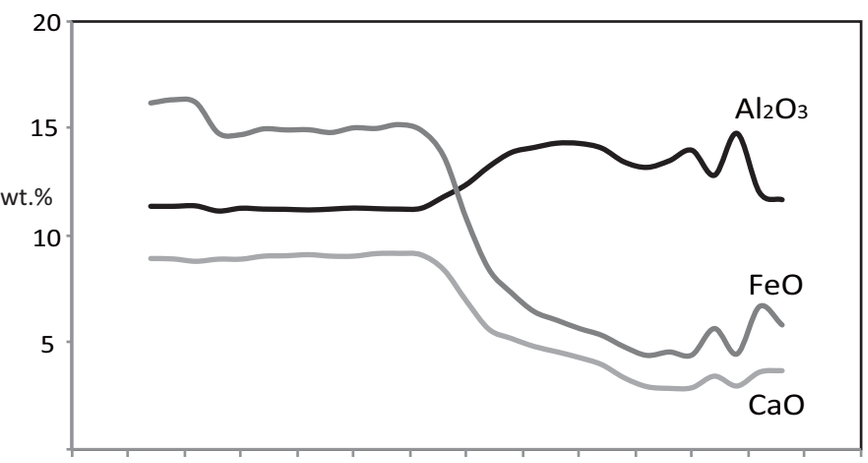
Al2O3
FeO
CaO
wt.%
20
15
10
5

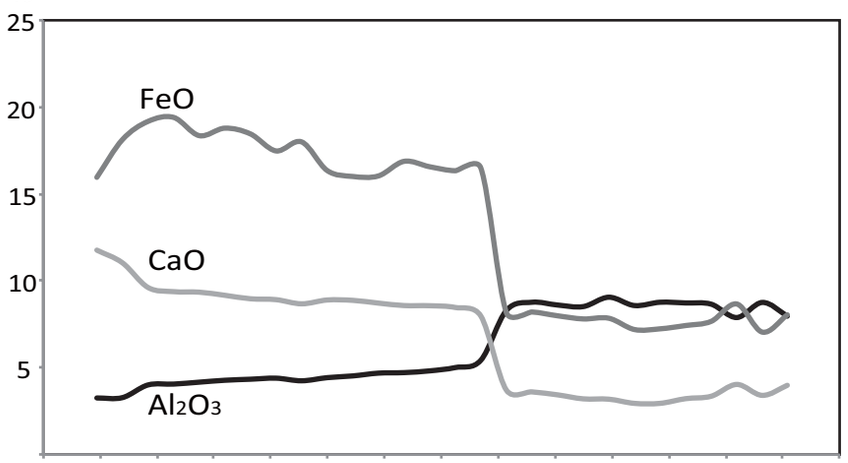
FeO
CaO
Al2O3
25
20
15
10
5

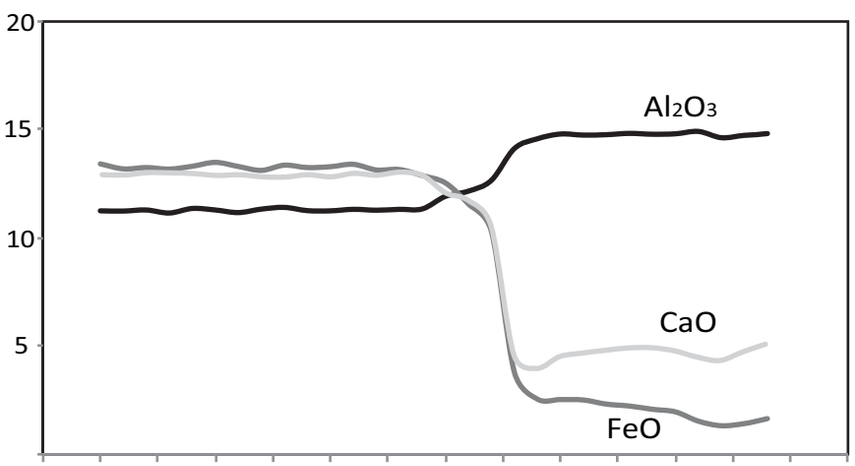
Al2O3
CaO
FeO
20
15
10
5

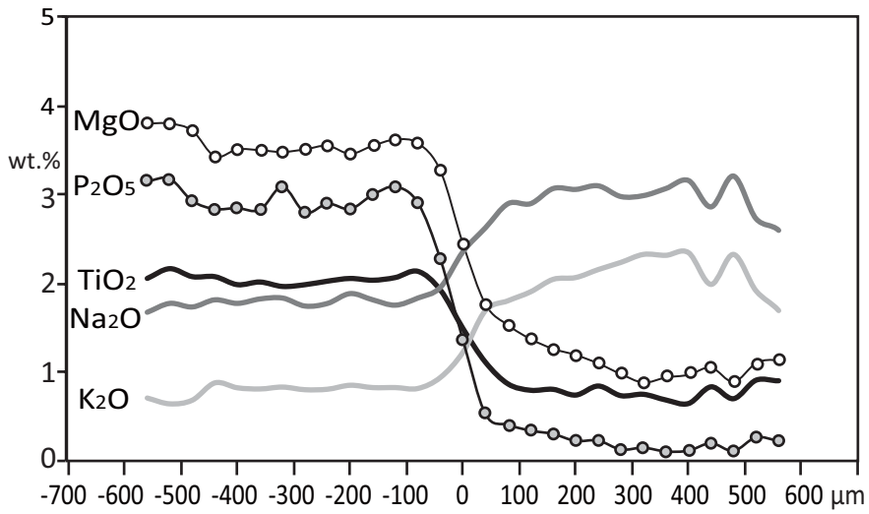
MgO
P2O5
TiO2
Na2O
K2O
wt.%
5
4
3
2
1
0
-700 -600 -500 -400 -300 -200 -100 0 100 200 300 400 500 600 µm

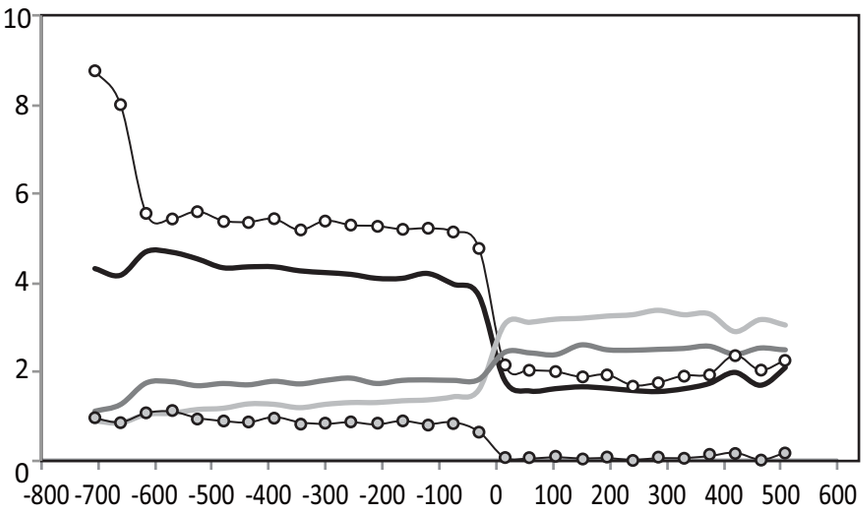
10
8
6
4
2
0
-800 -700 -600 -500 -400 -300 -200 -100 0 100 200 300 400 500 600

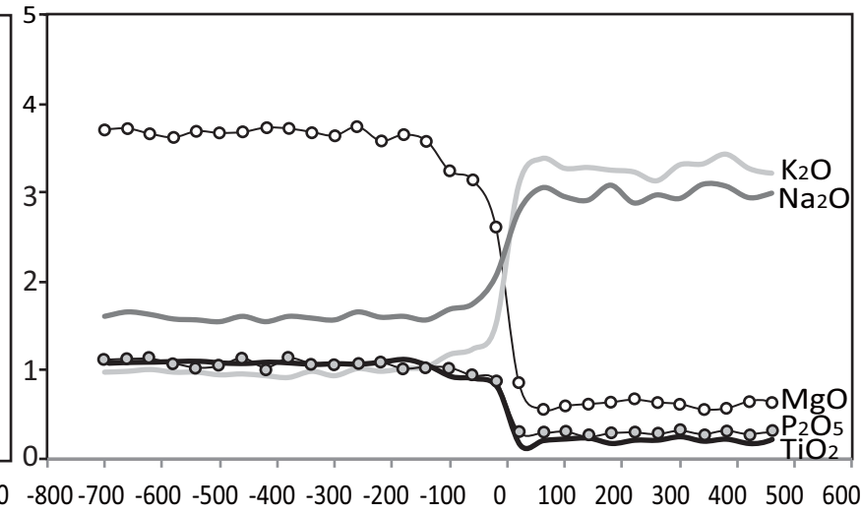
K2O
Na2O
MgO
P2O5
TiO2
5
4
3
2
1
0
-800 -700 -600 -500 -400 -300 -200 -100 0 100 200 300 400 500 600

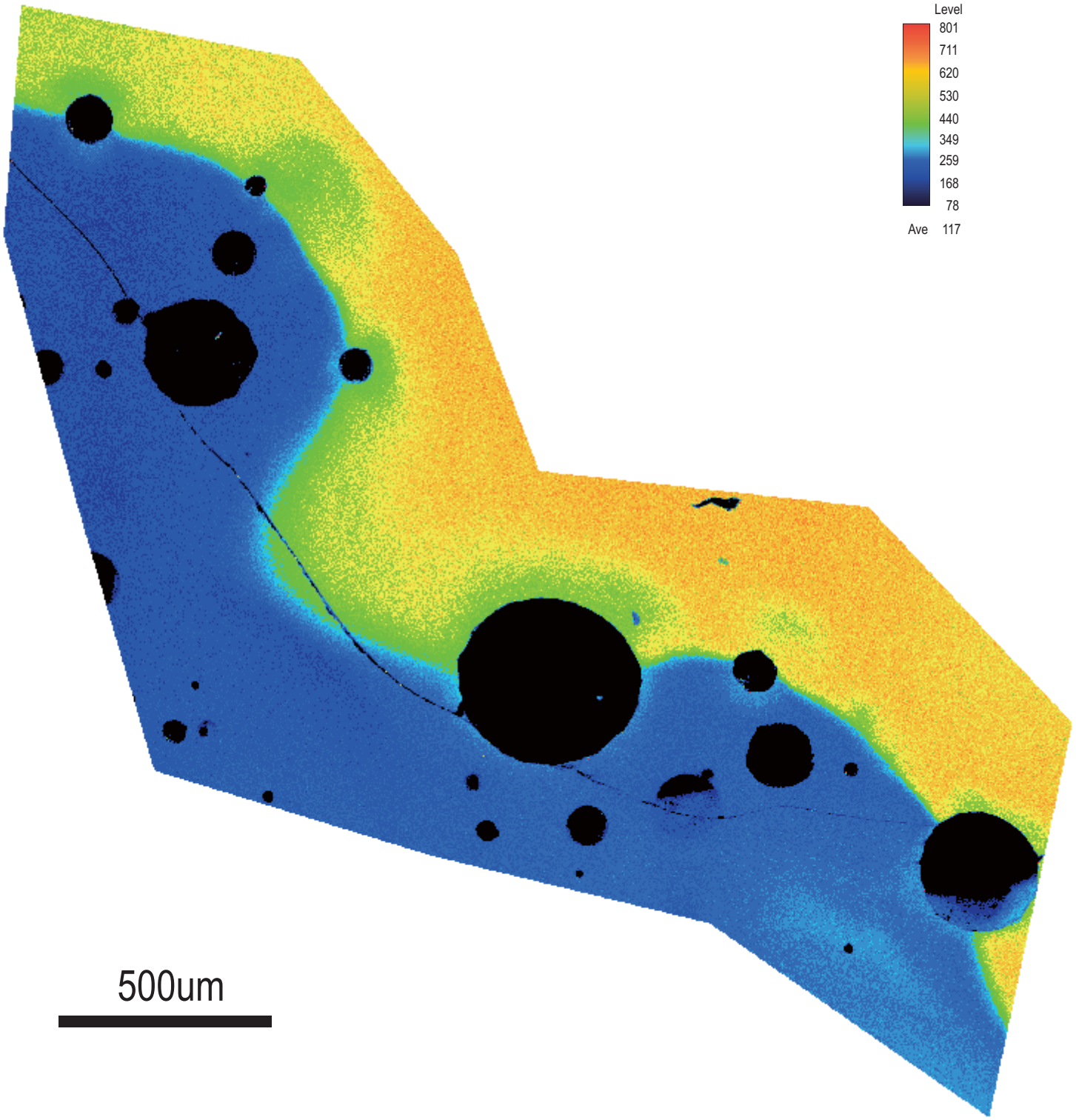
Level
801
711
620
530
440
349
259
168
78
Ave 117
500um

Table 1. Compositions of synthetic starting mixtures normalized to 100 wt.%.

Sample	MZ[a]		RY[b]		KC[c]		PZH[d]	
Phase	*Lfe*	*Lsi*	*Lfe*	*Lsi*	*Lfe*	*Lsi*	*Lfe*	*Lsi*
SiO_2	45.66	64.56	38.40	72.50	49.86	71.82	43.38	71.31
TiO_2	5.41	1.80	3.50	0.80	4.45	1.63	1.46	0.25
Al_2O_3	9.78	13.25	8.20	15.20	2.93	8.50	9.03	14.84
MgO	4.15	2.32	6.60	1.00	6.79	2.02	5.59	0.65
FeO	21.00	7.39	20.00	4.50	22.07	7.62	20.97	2.82
CaO	10.65	6.34	14.00	1.39	9.96	2.98	16.68	5.26
Na_2O	2.44	2.81	1.00	2.90	1.95	2.45	1.14	2.89
K_2O	0.48	1.37	0.30	1.70	0.96	2.98	0.31	2.31
P_2O_5	0.43	0.15	8.00	0.00	1.03	0.00	1.44	0.26
Total	100.0	100.0	100.0	100.0	100.0	100.0	100.0	100.0

Notes:Lfe, Fe-rich glass; *Lsi*, silicic glass.

[a.] Immiscible pairs produced by the centrifuge experiments of Veksler et al. (2007), where the starting composition is based on estimates of the liquid composition at the top of the Lower Zone of the Skaergaard layered intrusion.

[b.] Natural immiscible liquids in melt inclusions (quenched glasses) in native iron (c.f. Veksler et al. 2007).

[c.] Natural immiscible liquids (quenched glasses) in mesostasis of basaltic lavas (c.f. Veksler et al. 2007).

[d.] Natural immiscible liquids in melt inclusions hosted in apatite from the Middle Zone of the Panzhihua layered intrusion, China (Wang et al. 2013).

Table 2. Representative compositions of experimental products based on electron microprobe analyses of quenched glasses.

Sample	MZ1150	MZ1200	RY1150		RY1200		KC1150		KC1200		PZH1150		PZH1200	
T(°C)	1150	1200	1150		1200		1150		1200		1150		1200	
Phase	*L(N=3)*	*L(N=3)*	*Lfe(N=3)*	*Lsi(N=3)*	*Lfe(N=3)*	*Lsi(N=3)*	*Lfe(N=3)*	*Lsi(N=3)*	*Lfe(N=3)*	*Lsi(N=3)*	*Lfe(N=3)*	*Lsi(N=2)*	*Lfe(N=3)*	*Lsi(N=3)*
SiO_2	54.86	55.16	52.89	71.27	54.23	68.87	53.31	70.81	56.00	71.05	54.50	69.32	54.34	71.17
	(1.29)	(1.31)	(1.17)	(1.28)	(1.25)	(1.13)	(1.20)	(1.25)	(1.36)	(1.26)	(1.27)	(1.16)	(1.26)	(1.27)
TiO_2	3.93	4.02	2.05	0.79	2.01	1.09	4.39	1.90	4.22	1.72	1.01	0.27	1.09	0.28
	(0.20)	(0.20)	(0.10)	(0.12)	(0.10)	(0.05)	(0.12)	(0.10)	(0.21)	(0.09)	(0.05)	(0.01)	(0.05)	(0.01)
Al_2O_3	13.76	12.92	11.37	12.81	11.92	14.69	3.52	8.21	4.45	8.48	11.37	14.34	11.26	14.72
	(1.24)	(1.16)	(1.02)	(1.15)	(1.07)	(1.32)	(0.32)	(0.74)	(0.22)	(0.42)	(0.57)	(0.72)	(0.56)	(0.74)
FeO	8.39	8.38	16.25	5.65	14.72	4.00	17.76	7.92	16.21	7.29	12.88	3.35	13.29	1.46
	(0.17)	(0.17)	(0.33)	(0.56)	(0.29)	(0.31)	(0.36)	(0.40)	(1.46)	(0.66)	(1.16)	(0.30)	(1.20)	(0.13)
MgO	4.18	4.22	3.72	1.01	3.57	1.76	7.45	2.22	6.13	2.21	3.50	0.73	3.71	0.64
	(0.21)	(0.22)	(0.19)	(0.15)	(0.18)	(0.09)	(0.37)	(0.11)	(0.31)	(0.11)	(0.18)	(0.04)	(0.19)	(0.03)
CaO	9.27	9.19	8.87	3.42	8.27	3.99	10.81	3.81	9.44	3.85	12.45	5.09	12.80	5.25
	(0.46)	(0.45)	(0.44)	(0.47)	(0.41)	(0.20)	(0.20)	(0.19)	(0.47)	(0.19)	(0.62)	(0.25)	(0.64)	(0.26)
K_2O	0.79	0.77	0.64	1.94	0.73	1.64	0.91	3.03	1.15	3.10	1.02	3.44	0.99	3.31
	(0.04)	(0.04)	(0.06)	(0.04)	(0.05)	(0.03)	(0.05)	(0.15)	(0.06)	(0.08)	(0.05)	(0.07)	(0.05)	(0.07)
Na_2O	3.65	4.02	1.68	2.81	1.89	3.03	1.36	2.45	1.56	2.46	1.54	2.81	1.63	3.01
	(0.18)	(0.18)	(0.08)	(0.07)	(0.08)	(0.15)	(0.07)	(0.05)	(0.08)	(0.05)	(0.08)	(0.06)	(0.08)	(0.06)
P_2O_5	0.22	0.21	3.04	0.16	2.79	0.63	0.94	0.10	0.86	0.05	0.97	0.28	1.13	0.31
	(0.02)	(0.02)	(0.06)	(0.02)	(0.04)	(0.05)	(0.08)	(0.02)	(0.10)	(0.01)	(0.05)	(0.05)	(0.05)	(0.02)

Total	99.09	98.92	100.5	99.87	100.1	99.69	100.44	100.46	100.02	100.19	99.22	99.62	100.23	100.14

Note:

N represents the number of the analyses points of the immiscible phases that are away from the contact zone, and the composition is an average of these analyses. *Lfe,* Fe-rich glass; *Lsi*, silicic glass. Standard deviations are in parentheses